

# Common CNN-based Face Embedding Spaces are (Almost) Equivalent

David McNeely-White

Benjamin Sattelberg

Nathaniel Blanchard

Ross Beveridge

Colorado State University

Fort Collins, Colorado, USA

{david.white, ben.sattelberg, nathaniel.blanchard, ross.beveridge}@colostate.edu

## Abstract

CNNs are the dominant method for creating face embeddings for recognition. It might be assumed that, since these networks are distinct, complex, nonlinear functions, that their embeddings are network specific, and thus have some degree of anonymity. However, recent research has shown that distinct networks' features can be directly mapped with little performance penalty (median 1.9% reduction across 90 distinct mappings) in the context of the 1,000 object ImageNet recognition task. This finding has revealed that embeddings coming from different systems can be meaningfully compared, provided the mapping. However, prior work only considered networks trained and tested on a closed set classification task. Here, we present evidence that a linear mapping between feature spaces can be easily discovered in the context of open set face recognition. Specifically, we demonstrate that the feature spaces of four face recognition models, of varying architecture and training datasets, can be mapped between with no more than a 1.0% penalty in recognition accuracy on LFW. This finding, which we also replicate on YouTube Faces, demonstrates that embeddings from different systems can be readily compared once the linear mapping is determined. In further analysis, fewer than 500 pairs of corresponding embeddings from two systems are required to calculate the full mapping between embedding spaces, and reducing the dimensionality of the mapping from 512 to 64 produces negligible performance penalty.

## 1. Introduction

Convolutional Neural Networks (CNNs) are the state-of-the-art for embedding faces to represent individuals in biometrics applications, with many achieving well over 99% accuracy on face recognition benchmark datasets [6, 12, 26, 32]. There are a variety of network architectures and training methodologies used for constructing these embeddings, and much of the modern research focuses on enhancing

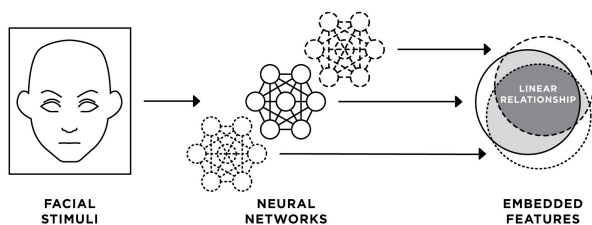


Figure 1: Face recognition systems often employ convolutional neural networks (CNNs) for feature embeddings. We find that multiple CNNs of varying architecture, training loss, and training dataset create embeddings which are nearly equivalent to one another via linear transformation. Using relatively few corresponding embeddings from these networks, linear mappings can be constructed which reliably convert one CNN's features into another's. Specifically, these mappings facilitate open-set face verification on LFW with at most a 1.0% penalty in accuracy when compared to their host network. We confirm our findings generalize to YouTube Faces.

ing those structures in ways that improve accuracy. Others have investigated what information these feature vectors encode and when they may be similar [1, 2, 20, 22]. What is not well understood, however, is whether embeddings from one network can be meaningfully compared to embeddings from other networks. It is straightforward to understand that direct distance-based comparisons are likely useless, since at a minimum, even if two networks converged on the same individual features, nothing about common training protocols prevents one encoding from being a permutation of the other. Further, this simple issue of permuted features does not even touch the deeper issue of some underlying equivalence.

The question of equivalent, or comparable, feature embeddings leads naturally to the question of whether there

is some discoverable mapping that facilitates comparison. Such mappings have already been shown to exist in a related context [15, 16], namely CNNs trained on and applied to the 1,000 object ImageNet dataset. Specifically, McNeely-White [16] demonstrated that an approximate linear mapping could be calculated from a set of corresponding feature vectors from two CNNs. Further, an exact linear mapping can be calculated directly from the actual weights in the input to the softmax layer of the two CNNs.

CNN generation for face recognition differs from the ImageNet [23] context in several important ways. For example, face embeddings often incorporate varying feature normalization constraints along with training loss functions, such as center loss, which might destroy linear mappings between networks. Further, after training face systems typically use a distance-based nearest-neighbor process to accomplish open-set face identification and verification. Put simply, while CNNs applied to ImageNet rely upon an unchanging set of 1,000 object labels, by design, CNNs for face recognition must generalize to an entirely new set of instances (i.e. people). Given these differences, as well as others, testing whether the basic findings by McNeely-White *et al.* [15, 16] extend to faces is important. This paper presents such tests along with findings indicating mappings are easily discovered between four distinct face-recognition CNNs. In addition, by using these mappings, face vectors from one may be directly compared to vectors from another. Figure 1 provides an overview of both our approach and findings.

The implications of our findings are broad, and of practical importance. One particularly practical implication concerns privacy. In essence, consider this potential method for determining the identity of an individual from an unlabeled embedding. First, obtain roughly 400 paired face vectors, one from the same system which generated the unlabeled embedding along with corresponding vectors from a known system and use these to calculate the mapping between embeddings. Next, use this mapping to create a version of the unlabeled embedding which may be used to retrieve the unknown identity from the second system’s enrollment set. The implications are significant for anyone assuming that a nonlinear CNN-based embedding system is adequate to obfuscate individual identities; for example, the privacy-conscious face re-identification system proposed by Seyed Ali Miraftebade *et al.* [17].

The remainder of this paper is organized as follows. Section 2 covers others’ related work studying the features of face recognition systems, including feature fusion and transfer learning. Section 3 describes the datasets and networks we used, in addition to our experimental methodology. Section 4 presents our results applying our linear mappings and our analysis of these mappings.

## 2. Related Work

In this work we study feature embeddings of face recognition models. Others have studied feature embeddings for various purposes also. These embeddings or vectors are usually the output of final layers of neural networks trained to cluster images [6, 26, 30]. Indeed, the dot product of two images’ normalized embeddings is often used as a similarity score to rank the likelihood that they are of the same person [6, 30]. Note that these measures are often grouped under the heading “cosine distance.”

Early on, neural network implementations did not generalize well across domains, failing when presented with confounding factors such as illumination [22]. With the introduction of richer training datasets, neural networks generalize better, and achieved high performance on complex evaluation datasets [26, 33]. It has also been established that these feature embeddings contain information about image features such as the angle of view of the face, media type, or position of the face in the image [4, 20]. Still, while neural networks now encode information about these variations in images, and tend to generalize across them, it has been noted that the feature embeddings of different networks can encode information differently, such as pose, illumination, and local features [2]. Indeed, others have found that the feature embedding spaces of networks also cluster in certain semantic ways beyond just identity, such as by gender, ethnicity, and illumination [9]. This gap in encoded information has been exploited by various methods including feature fusion. By combining the feature encodings from two different networks, it has been shown in some cases that facial recognition accuracy can be improved significantly [1, 2]. What’s more, some have created mappings within a given feature space which effectively reduce large pose variations [4]. We also consider feature embeddings, but we create mappings between networks which simply encode the differences between embedding spaces.

In another direction, some have investigated what effect certain model choices have on feature quality and robustness. Fine-tuned models have been shown to generate better features for the related task of iris recognition [3]. Various hyperparameter choices, such as data augmentation, architecture, and choice of layer to take embeddings from have been investigated for their efficacy in generating features from deep CNNs [29]. The differences in accuracies found by these studies further suggests that feature embeddings from different networks will encode different information. We also analyze features, but, in contrast to these efforts, we find similarities in features, though we compare across networks.

Others research shows that the feature spaces are able to be greatly compressed — standard feature spaces of dimension 512 or 1024 contain enough degrees of freedom to fully encode every human face, and typically the di-

mension of these spaces can be reduced by up to 10 times with only minor drops in accuracy [20]. Sixue Gong *et al.* [8] has demonstrated similar results also, compacting 512-dimension SphereFace [14] embeddings to 16 dimensions with moderate performance penalty. In Sections 4.1 and 4.2, we find that relatively little information is necessary to generate high quality mappings, which may be due to the same effects studied by these works.

As mentioned in the introduction, networks trained on ImageNet have been shown to have near linear-equivalent pre-logit feature spaces [15, 16]. This prior work shares a number of similarities to our own, but we expand upon those works by considering a different domains and other network architectures. The ILSVRC2012 dataset is an image-classification system and the networks considered by McNeely-White *et al.* [15, 16] did not strictly use feature embeddings for classification as with common face recognition models. Their models also were not trained to generate feature embeddings, and so share a strong relationship simply by their common logit space.

Both the work we present here and transfer learning share an underlying concern for how feature spaces behave in response to changes in training and testing and transfer learning has been shown to be applicable to various face-related tasks [7, 18, 19]. However, where transfer learning adapts an existing model successful in one domain to a different domain, the work presented here keeps the domain fixed and instead explores the differences between feature spaces generated by different networks.

### 3. Methods

In this section, we first introduce the datasets (3.1) and networks (3.2) used in our experiments. We then detail the methods used for fitting (3.3) and analyzing mappings (3.4).

#### 3.1. Datasets

As listed in Table 1, we use four face datasets: VGGFace2 [5], CASIA-WebFace [33], MS-Celeb-1M [10], and Labeled Faces in the Wild (LFW) [12]. A key research question our experiments address is whether face feature

Dataset	# individuals	# images
VGGFace2	9131	3.31 M
CASIA-WebFace	10,575	494,414
MS-Celeb-1M	100,000	10 M
LFW	5,749	13,233
YouTube Faces	1,595	3,425 videos

Table 1: The datasets used in our experiments. The first three datasets were used to train networks used in our experiments. The fourth, LFW, was used to test mappings between feature spaces.

vectors obtained by networks trained on different individuals are comparable, and comparable within an open set context. Therefore the VGGFace2, CASIA-WebFace, and MS-Celeb-1M datasets were used for training, as more fully described in Section 3.2. The LFW dataset is reserved for all comparisons of recognition performance using different feature space mappings.

#### 3.1.1 Training Datasets

VGGFace2 is composed of images drawn from Google Image Search; it comprises 3.31 million images of 9,131 subjects. The goal of the dataset was to have a large number of images and subjects that cover a variety of attributes while minimizing label noise [5].

CASIA-WebFace consists of 494,414 images of around 10,575 subjects. It is composed of photos of celebrities born between 1940 and 2014, drawn from the IMDB website, and is intended for use in training algorithms to be evaluated on LFW [33].

MS-Celeb-1M (also MS1M) is a dataset of 10 million images of 100,000 celebrity subjects. At time of its publication, it was the largest publicly available face dataset [10].

#### 3.1.2 LFW

LFW contains 13,233 images of 5,749 people along with a well defined and simple evaluation protocol.

Name	CNN	Loss function	Training Dataset	Accuracy on LFW	Accuracy on YTF
<b>Model-IC</b>	InceptionResNetV1	Softmax + Center	CASIA-WebFace	99.03% ± 0.42%	92.49% ± 1.13%
<b>Model-IV</b>	InceptionResNetV1	Softmax + Center	VGGFace2	99.47% ± 0.37%	95.51% ± 1.05%
<b>Model-MM</b>	MobileNetV2	ArcFace	MS-Celeb-1M	98.70% ± 0.50%	86.64% ± 1.55%
<b>Model-RM</b>	ResNet50V2	ArcFace	MS-Celeb-1M	99.40% ± 0.46%	91.20% ± 0.96%

Table 2: Configuration and accuracy of each model. A shortened name is provided for use in other tables. Note these accuracy values are calculated by internal verification and differ from the stated values for each model’s source publication (note also that these models are not the official standards associated with the publications).

The protocol involves 10 pre-determined subsets of matching and non-matching image pairs to be evaluated using in 10-fold cross validation. Each fold’s similarity threshold is determined over the nine training subsets and that threshold is used for calculating the accuracy on the remaining validation fold. Following this now very commonly used protocol below we will be reporting average accuracy over these 10 folds [12]. Generally, it is recognized that overall performance on LFW is very high, leaving little room for absolute improvement. However, what we need is a well understood dataset on which we can quantify recognition accuracy drops when mapping between feature spaces. For this purpose LFW is a good choice.

### 3.1.3 YouTube Faces

YouTube Faces (YTF) [31] contains 3,425 videos of 1,595 people and an evaluation protocol similar to LFW. There are an average of 181.3 frames per video.

As with LFW, 10 pre-determined subsets of matching and non-matching video pairs are evaluated using 10-fold cross validation. When comparing videos, it is common to either average the embeddings for the first 100 frames, and use the resulting single average embedding in place of the video [30, 6]. Other approaches include averaging the similarity between all pairs of frames [26]. Again, similarity thresholds are determined over the 9 training subsets, and accuracy at that threshold is reported over the remaining validation fold.

YTF provides a dataset for determining set-to-set accuracy that requires a stronger ability for models to be invariant to pose or occlusions due to the video format. In contrast to LFW, it provides a dataset that is more difficult for the models to determine how well our mapping results generalize to more complex data.

## 3.2. Networks

We use four pre-trained face recognition CNNs obtained from two open-source GitHub repositories, as described both below and in Table 2. All four networks generate feature embeddings in  $\mathbb{R}^{512}$  and achieve greater than 99% accuracy on LFW. The first two were trained using center loss on CASIA-WebFace and VGGFace2. The second two were trained using ArcFace loss on MS-Celeb-1M. It should be noted that prior work has demonstrated that it is not necessary for the number of dimensions per model to match [15, 16].

The first two networks use center loss for training, which is a loss function designed to work alongside softmax loss. The goal of this loss function is to cluster features belonging to the same class together, in addition to the separation of classes that softmax loss gives. During training, each class has an associated center that is moved as the feature

embedding space changes. The center loss for a given input image is calculated as the distance from its feature embedding to the associated class center. Total loss is calculated as the sum of the center and softmax losses. Wen *et al.* [30] experimentally demonstrated that center loss outperforms softmax loss by itself, and methods such as triplet loss [26] that are commonly used for face verification (accuracy = 99.28% on LFW, 94.9% on YTF).

We consider two networks trained with center loss and a softmax classifier, both trained by David Sandberg and available on GitHub<sup>1</sup> [24]. Both of those models use the same CNN architecture, starting with a multi-task CNN (MTCNN) to align faces, which are converted to feature embeddings via an Inception-ResNet-v1 [27] CNN, before being mapped to the unit hypersphere via L2-normalization. The CNNs were trained using a softmax classifier with combined cross-entropy and center loss on the normalized features. Training also involves data augmentation through random image crops and flips. One of these models (Model-IC) was trained on CASIA-WebFace and achieves an accuracy of 99.05% on LFW and the other (Model-IV) was trained on VGGFace2 and achieves an accuracy of 99.65% on LFW as reported in their GitHub repository [24].

We consider two networks trained with ArcFace loss, both trained by Kuan-Yu Huang and available on GitHub<sup>2</sup>[13]. Faces are again aligned using an MTCNN, then passed into either MobileNet-v2 [25] or ResNet50-v2 [11]. Training loss is calculated from the resulting feature embeddings via cross-entropy loss using a softmax classifier, including an additive angular margin penalty as described by the ArcFace authors [6]. ArcFace loss is another, more recent, loss function designed to address shortcomings of softmax and triplet loss. It is a modification of softmax loss to constrain feature embeddings to the unit-hypersphere and emphasize the angle between data points rather than the Euclidean distance between them. The authors report a 99.53% accuracy on LFW and 98.02% on YTF [6]. During inference, embeddings are generated then normalized. Training also involves data augmentation through random image flips and crops as well as randomized saturation and brightness adjustments. The MobileNet-v2 model (Model-MM) trained on MS-Celeb-1M achieves 99.35% accuracy on LFW, and the ResNet50-v2 model (Model-RM) trained on MS-Celeb-1M achieves 98.67% accuracy as stated in their GitHub repository [13].

These pre-trained models are used to generate pairs of feature embeddings over all 6,000 image pairs specified in the LFW dataset [12] and 5,000 video pairs specified in the YTF dataset [31]. In the case of YTF, a single embedding per video is produced by averaging the embeddings produced from the first 100 frames. Accuracy is measured by

<sup>1</sup><https://github.com/davidsandberg/facenet>.

<sup>2</sup><https://github.com/peteryuX/arcface-tf2>.

performing 10-fold cross-validation on aligned image embeddings as specified by the *Image Restricted, labeled outside data* protocol documented in LFW and YTF [12, 31] and previously in Section 3.1.2. Specifically, for each fold a cosine distance threshold is found which maximizes accuracy (i.e. labels the most image pairs correctly as matched or mismatched) over nine training partitions. Using the remaining validation partition, accuracy is measured using the same threshold. This process is repeated for each of 10 folds given by the LFW dataset in `pairs.txt` and the YTF dataset in `pairs.csv` and averaged to produce a final accuracy measurement.

All four models were internally validated to within 0.01% of stated accuracies on LFW. However, the margin between stated accuracies and internal validation is much larger using YTF, likely due to differences in image preprocessing. See Table 2 for model descriptions and the accuracies we reproduced internally. Additional training details such as learning rate schedules, optimizers, and specific software details are documented at the source repositories. Importantly, each model differs from another by either architecture, dataset, or both.

### 3.3. Fitting Linear Maps

We are interested in seeing how well the feature embeddings of one source network are able to replicate the embeddings of another target network. To do this, we generate linear mappings that transform the feature embedding space of a source network to the feature embedding space of a target network. These linear mappings are fit during the LFW/YTF evaluation process using a process similar to that described in [15, 16] and detailed below. Importantly, linear mappings were chosen since they demonstrate the simplicity of the relationship between embedding spaces, if successful.

During the evaluation of one fold of LFW or YTF, the set of matched image pairs that have both images representing the same individual,  $(x_i, y_i), i = 1, \dots, m$ , from the nine training folds are used as training data for fitting the linear mapping. For reference, each LFW fold contains 300 matched and 300 mismatched pairs, so  $m = 9 * 300 = 2,700$ . Then, we can use the source network,  $f_1 : \text{image space} \rightarrow \mathbb{R}^{512}$ , and the target network,  $f_2 : \text{image space} \rightarrow \mathbb{R}^{512}$  to construct the matrices of feature embeddings

$$\mathbf{S} = \begin{bmatrix} f_1(x_1)^T \\ \vdots \\ f_1(x_m)^T \end{bmatrix} \text{ and } \mathbf{T} = \begin{bmatrix} f_2(y_1)^T \\ \vdots \\ f_2(y_m)^T \end{bmatrix}. \quad (1)$$

These  $\mathbf{S}$  and  $\mathbf{T}$  matrices are used to train a ridge regression classifier in Python’s scikit-learn package [21] that minimizes

$$\|\mathbf{S} * \mathbf{M} - \mathbf{T}\|_2^2 + \|\mathbf{M}\|_2^2 \quad (2)$$

for the mapping matrix  $\mathbf{M} \in \mathbb{R}^{512 \times 512}$ .

Then, given this mapping, we can calculate the cosine distance between two images,  $x$  and  $y$ , as

$$d(x, y) = 1 - \frac{(f_1(x)^T * M) \cdot f_2(y)}{\|f_1(x)^T * M\|_2 * \|f_2(y)\|_2}. \quad (3)$$

The distance  $d$  is used to calculate an optimal threshold,  $\tau$ , for the training folds, which is then used with  $d$  to determine if a pair of images are of the same individual on the validation fold, as is standard for LFW. This process is demonstrated in Figure 2.

### 3.4. Sensitivity to Number of Corresponding Pairs

To better understand the amount of correspondence necessary to create these mappings, we also perform a sensitivity analysis using LFW. This involves the same process as described previously, but rather than using all 2,700 matching pairs, we sample a subset of  $1 \leq p \leq m$  of them for fitting the linear map. We perform this during each fold simply by randomly selecting the  $p$  training pairs from all of the matching pairs available, and calculating the mean accuracy over all folds for that number of pairs. By recording the accuracy achieved using fewer pairs for training at each fold, we are able to discern the number of corresponding pairs necessary to reliably map between embedding spaces. We record the accuracy achieved for 100 values of  $p$  distributed uniformly between 1 and 2,700.

## 4. Results

The accuracies for each mapping fit are shown in Tables 3 and 4. The loss in accuracy introduced by linear mapping is at most 1.0% for LFW, and 13.9% for YTF. In our experiments, Model-MM is outperformed by other models by a large margin, which may account for the poor performance of mappings to and from its feature space. Indeed, excluding Model-MM reduces the maximum mapping performance penalty on YTF by more than half. Further, the images in YTF are generally lower quality due to motion blur or distance, which may account for greater disparities in performance. Regardless, the ability for one network’s features to robustly replicate another’s demonstrates a near-linear equivalence of the feature spaces. Although some information does not transfer, the vast majority of information that is encoded by each network is equivalent. This finding is in contrast to previous results that methods such as feature fusion increase the accuracy of the networks [1, 2]. However, we note that the small amount of information not encoded by this linear transform may result in the increases in accuracy revealed in those experiments.

We also consider the case where  $M$  is the identity mapping in order to demonstrate that the embeddings generated by the four networks are not directly comparable. In this

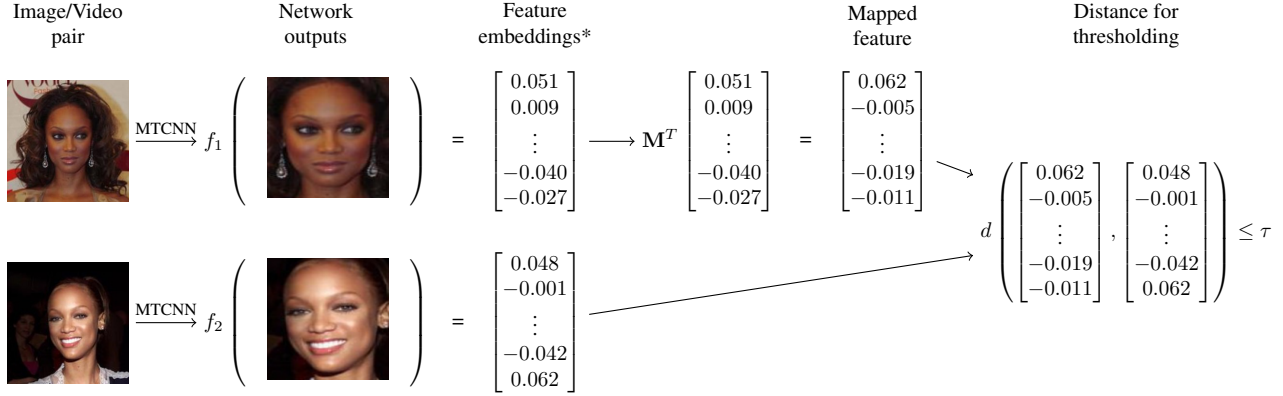


Figure 2: The pipeline used for evaluating the linear mappings. Both networks use separate multi-task CNNs (MTCNN) to detect and align the faces. The networks are then used to generate feature embeddings in  $\mathbb{R}^{512}$ . The linear mapping is used to map the feature embedding of the source network ( $f_1$ ) into the feature space of the target network ( $f_2$ ). Finally, the distance  $d$  between the embeddings is computed and compared against the matching threshold  $\tau$ ; often distance is simply one minus the cosine of the angle between embedding vectors. \*In the case of YTF, embeddings are generated for the first 100 frames of the video, then averaged to produce a single embedding per video.

		To			
		Model-IC	Model-IV	Model-MM	Model-RM
From	Model-IC	<b>99.03%</b>	<b>98.98%</b> (58.12%)	<b>98.32%</b> (51.78%)	<b>98.67%</b> (51.00%)
	Model-IV	<b>98.82%</b> (57.03%)	<b>99.47%</b>	<b>98.63%</b> (52.42%)	<b>98.48%</b> (52.25%)
	Model-MM	<b>98.07%</b> (50.30%)	<b>98.50%</b> (51.88%)	<b>98.70%</b>	<b>98.32%</b> (51.62%)
	Model-RM	<b>98.60%</b> (52.45%)	<b>98.78%</b> (52.95%)	<b>98.52%</b> (52.43%)	<b>99.40%</b>

Table 3: The accuracy of each network when mapped, using LFW. Diagonal elements correspond to the unmodified accuracy of each model (see Table 2). Off-diagonal elements correspond to the accuracy obtained when comparing features across networks, with the “From” model’s features mapped by linear transformation to approximate the “To” model’s features. The maximum drop in accuracy introduced by any mapping is 1.0%. The number in parentheses indicates the performance when comparing embeddings across networks directly—without mapping. Note that for the LFW validation set, 50% accuracy corresponds to random chance.

		To			
		Model-IC	Model-IV	Model-MM	Model-RM
From	Model-IC	<b>92.49%</b>	<b>93.60%</b> (57.27%)	<b>84.69%</b> (50.49%)	<b>88.36%</b> (51.33%)
	Model-IV	<b>88.73%</b> (55.82%)	<b>95.51%</b>	<b>81.58%</b> (50.09%)	<b>86.29%</b> (50.04%)
	Model-MM	<b>83.07%</b> (50.43%)	<b>89.31%</b> (50.89%)	<b>86.64%</b>	<b>86.04%</b> (51.02%)
	Model-RM	<b>86.82%</b> (50.31%)	<b>90.80%</b> (50.09%)	<b>84.18%</b> (50.09%)	<b>91.20%</b>

Table 4: The accuracy of each network when mapped, using YTF. The format is identical to Table 3. The maximum drop in accuracy introduced by any mapping is 13.9% when mapping Model-IV’s embeddings into the embedding space of Model-MM.

case, as shown parenthetically in Tables 3 and 4, the accuracy drops drastically to nearly random (50% in these cases). Although, when converting between the two models trained using center loss, there is a non-trivial increase above random, suggesting that those two networks may have some features of their embedding space that are easy to translate between. The results of these experiments clearly show that the embedding spaces generated by all 4 models are separate and distinct when compared directly, but can be reliably converted using a simple linear transformation.

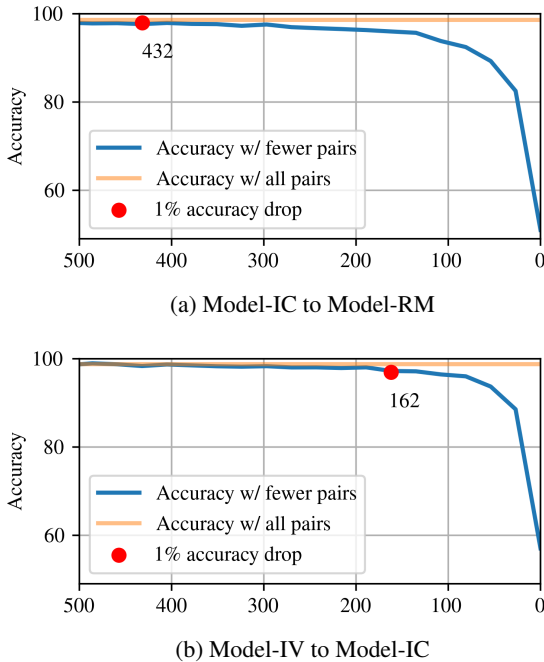


Figure 3: Quantifying how the number of corresponding pairs of embeddings available alters the quality of linear mapping for Model-IC mapped to Model-RM (a) and Model-IV mapped to Model-IC (b). The orange line indicates the mean accuracy achieved by mapping using all training pairs. The blue line shows the mean accuracy (y-axis) of this mapping using a reduced number of pairs (x-axis). The red dot shows the number of pairs which produce an accuracy drop of 1%. Note: while the number of training pairs available to the mapping is reduced, all pairs are included in the search for optimal distance threshold for use on the held-out test pairs.

#### 4.1. Sensitivity Results

The accuracy obtained by fitting mappings using a reduced number of corresponding image pairs is shown in Figure 3. This figure includes two selected mappings: Model-IC to Model-RM (Figure 3a) and Model-IV to Model-IC (Figure 3b). These two examples bound the

remaining mappings (i.e. they are the best- and worst-performing in terms of the number of pairs necessary to train a mapping that performs 1% worse as indicated by the red dot). Summarizing all such analyses, only about 200 to 400 image pairs are necessary to fit a mapping which performs 1% worse than one which uses all 2,700 pairs. This demonstrates that relatively little information is required to generate high-quality mapping, in contrast to the large (100,000+) number of samples necessary to train the embedding networks themselves. As discussed in Section 2, others have demonstrated that the underlying dimensionality of these spaces is much smaller than 512 [8, 20, 28], the small number of corresponding pairs required to generate a mapping still speaks to the simplicity of the relationship between feature spaces.

#### 4.2. Ablation

The embeddings generated by these models are 512-dimensional, but the actual data generated by the models is a subspace of  $\mathbb{R}^{512}$ . As described in Section 2, Sixue Gong *et al.* [8] showed that 512-dimension embeddings can be reduced to as few as 16 dimensions without significant decrease in representational ability on the underlying dataset.

Due to the nature of our mappings, we are able to analyze the dimensionality of the mapping between the subspaces by analyzing the mapping matrices.

We can investigate the dimensionality of our mappings to determine how the transformation of these subspaces is done. Specifically, although the mapping matrices are “full rank,” the singular values associated with these matrices have a steep dropoff. In most cases upwards of 99% of the variance of the mapping matrices is accounted for by the first 50 to 100 singular values. By calculating a singular value decomposition of the mapping matrices and truncating all but the largest singular values, we can construct lower rank approximations to the original mapping. As shown in Figure 4, there is very little reduction in accuracy until only 64 singular values are kept. In most cases, somewhat reasonable accuracy is maintained with as few as 16. This suggests that the embeddings being mapped between lie in low dimensional subspaces of the full embedding dimension, and that those subspaces can be mapped between linearly.

#### 5. Conclusion

We have established a linear near-equivalence between 4 face recognition CNNs: Model-IC, Model-IV, Model-MM and Model-RM, as reported in Table 2. Care was taken to vary the choice of architecture, the choice of loss function and the choice of training data. Given the differences between the four models, it is significant that all four CNNs generated feature vectors for faces which are nearly equivalent when the linear mapping between embedding spaces is



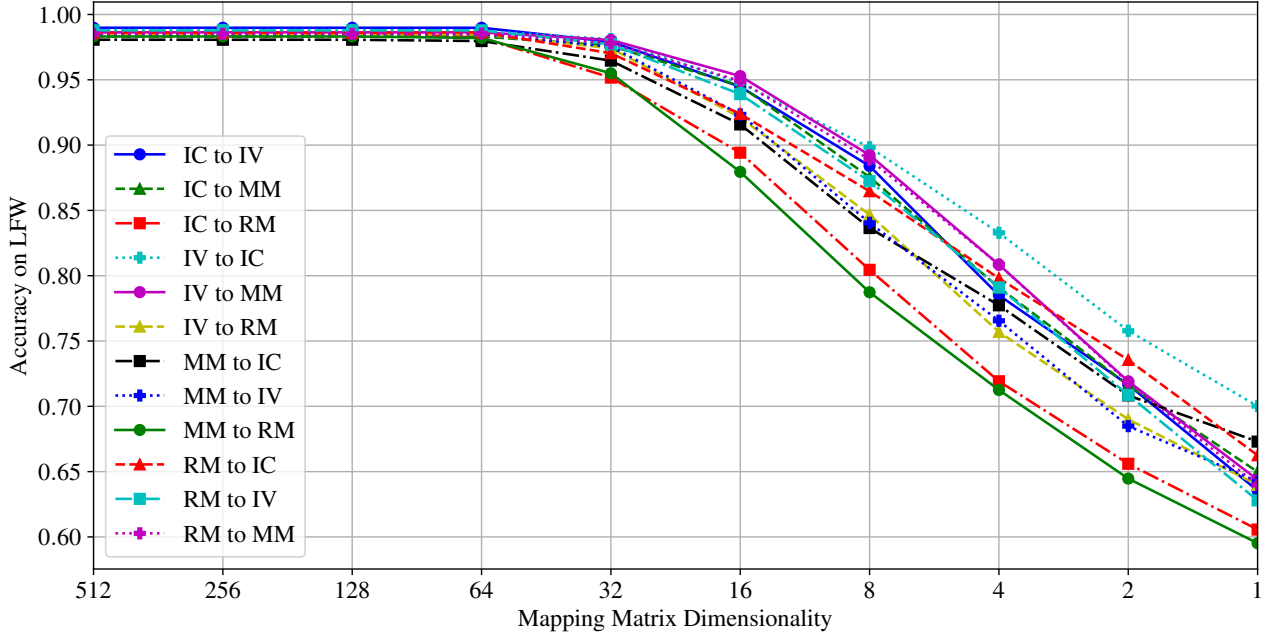


Figure 4: Quantifying the accuracy after mapping as the rank of the mapping matrix is reduced. Dimensionality reduction is achieved by truncating some number of the singular values in a singular value decomposition and using the resulting matrix for mapping. Results are shown for all mappings on LFW. Model-MM to Model-RM and Model-IC to Model-RM perform the worst, seeming to require a higher dimensionality to perform well.

calculated. The implications of this finding are clear and far-reaching: if multiple models of varying architecture, training dataset, and training loss produce features which can be accurately compared after only a linear transformation, it implies that there is a shared structure among each of their feature spaces. In other words, besides in the case of null spaces, a linear transformation is structure-preserving. This means that each of these feature spaces shares a common structure, despite no single common training dataset nor architecture. If this is indeed true of other CNNs trained on other face datasets, it implies that the structure of CNN feature spaces is dependent only on the task.

The existence of near linear equivalence between the embeddings spaces for these different CNNs has further practical implications. First, as already mentioned in the introduction, our findings represent a cautionary tale for any system designer who hopes to obfuscate an individual’s identity via CNN embeddings. By use of relatively few corresponding embeddings, embeddings generated from an unknown model may be compared to embeddings from potentially many other models. One could then conceivably compare unlabeled embeddings from the unknown source to labeled embeddings from another source to determine the identity of an individual. This strongly suggests that, like other forms of identity, the embedding generated from the face of a person should be stored in a secure manner.

While the implications for privacy might be viewed as

unfortunate, there are two positive implications. Namely, our findings suggest that interoperability between different face embedding standards may be a simpler task than it might at first appear. Indeed this implication can be taken further. What emerges from a view that different CNNs map to spaces which are easily moved between by use of linear operators is a broader picture, i.e. there is essentially one underlying embedding space. What CNNs are discovering is a particular variant of this underlying embeddings space. By this line of reasoning, it becomes interesting to speculate about what might be a means of capturing some quintessential canonical form for the embedding space.

Finally, perhaps the most interesting question we can close with is this: what will it mean when we start expanding our suite of machine learning models and associated embedding spaces so that we actually find an embedding space which does not have such a strong linear relationship with the rest? This gets to the heart of questions related to what is, and is not, common between machine learning models. For our part, we end with the suggestion that it may become routine to test for linear equivalence as part of the formal process of assessing the novelty and value of a new face recognition system.

## References

- [1] Ankan Bansal, Rajeev Ranjan, Carlos D Castillo, and Rama Chellappa. Deep features for recognizing disguised faces in



- the wild. In *Proceedings of the IEEE Conference on Computer Vision and Pattern Recognition Workshops*, pages 10–16, 2018.
- [2] Navaneeth Bodla, Jingxiao Zheng, Hongyu Xu, Jun-Cheng Chen, Carlos Castillo, and Rama Chellappa. Deep heterogeneous feature fusion for template-based face recognition. In *2017 IEEE winter conference on applications of computer vision (WACV)*, pages 586–595. IEEE, 2017.
- [3] Aidan Boyd, Adam Czajka, and Kevin Bowyer. Deep learning-based feature extraction in iris recognition: Use existing models, fine-tune or train from scratch? *arXiv preprint arXiv:2002.08916*, 2020.
- [4] Kaidi Cao, Yu Rong, Cheng Li, Xiaoou Tang, and Chen Change Loy. Pose-robust face recognition via deep residual equivariant mapping. In *The IEEE Conference on Computer Vision and Pattern Recognition (CVPR)*, June 2018.
- [5] Qiong Cao, Li Shen, Weidi Xie, Omkar M Parkhi, and Andrew Zisserman. Vggface2: A dataset for recognising faces across pose and age. In *2018 13th IEEE International Conference on Automatic Face & Gesture Recognition (FG 2018)*, pages 67–74. IEEE, 2018.
- [6] Jiankang Deng, Jia Guo, Niannan Xue, and Stefanos Zafeiriou. Arcface: Additive angular margin loss for deep face recognition. In *Proceedings of the IEEE Conference on Computer Vision and Pattern Recognition*, pages 4690–4699, 2019.
- [7] Mengyue Geng, Yaowei Wang, Tao Xiang, and Yonghong Tian. Deep transfer learning for person re-identification. *arXiv preprint arXiv:1611.05244*, 2016.
- [8] Sixue Gong, Vishnu Naresh Boddeti, and Anil K Jain. On the intrinsic dimensionality of image representations. In *Proceedings of the IEEE Conference on Computer Vision and Pattern Recognition*, pages 3987–3996, 2019.
- [9] Jason Grant and Patrick Flynn. Hierarchical clustering in face similarity score space. *arXiv preprint arXiv:1605.06052*, 2016.
- [10] Yandong Guo, Lei Zhang, Yuxiao Hu, Xiaodong He, and Jianfeng Gao. Ms-celeb-1m: A dataset and benchmark for large-scale face recognition. In *European conference on computer vision*, pages 87–102. Springer, 2016.
- [11] Kaiming He, Xiangyu Zhang, Shaoqing Ren, and Jian Sun. Identity mappings in deep residual networks. In *European conference on computer vision*, pages 630–645. Springer, 2016.
- [12] Gary B Huang, Marwan Mattar, Tamara Berg, and Eric Learned-Miller. Labeled faces in the wild: A database for studying face recognition in unconstrained environments. 2008.
- [13] Kuan-Yu Huang. Arcface unofficial implemented in tensorflow 2.0+ (resnet50, mobilenetv2)., June 2020.
- [14] Weiyang Liu, Yandong Wen, Zhiding Yu, Ming Li, Bhiksha Raj, and Le Song. Sphereface: Deep hypersphere embedding for face recognition. In *Proceedings of the IEEE conference on computer vision and pattern recognition*, pages 212–220, 2017.
- [15] David McNeely-White, J. Beveridge, and Bruce Draper. Inception and resnet features are (almost) equivalent. *Cognitive Systems Research*, 59, 10 2019.
- [16] David G McNeely-White. Same data, same features: Modern imagenet-trained convolutional neural networks learn the same thing. Master’s thesis, Colorado State University, 2020.
- [17] Seyed Ali Miraftebadeh, Paul Rad, Kim-Kwang Raymond Choo, and Mo Jamshidi. A privacy-aware architecture at the edge for autonomous real-time identity reidentification in crowds. *IEEE Internet of Things Journal*, 5(4):2936–2946, 2017.
- [18] P. Mittal, M. Vatsa, and R. Singh. Composite sketch recognition via deep network - a transfer learning approach. In *2015 International Conference on Biometrics (ICB)*, pages 251–256, 2015.
- [19] Hong-Wei Ng, Viet Dung Nguyen, Vassilios Vonikakis, and Stefan Winkler. Deep learning for emotion recognition on small datasets using transfer learning. In *Proceedings of the 2015 ACM on international conference on multimodal interaction*, pages 443–449, 2015.
- [20] Alice J O’Toole, Carlos D Castillo, Connor J Parde, Matthew Q Hill, and Rama Chellappa. Face space representations in deep convolutional neural networks. *Trends in cognitive sciences*, 22(9):794–809, 2018.
- [21] F. Pedregosa, G. Varoquaux, A. Gramfort, V. Michel, B. Thirion, O. Grisel, M. Blondel, P. Prettenhofer, R. Weiss, V. Dubourg, J. Vanderplas, A. Passos, D. Cournapeau, M. Brucher, M. Perrot, and E. Duchesnay. Scikit-learn: Machine learning in Python. *Journal of Machine Learning Research*, 12:2825–2830, 2011.
- [22] C. Ren, D. Dai, K. Huang, and Z. Lai. Transfer learning of structured representation for face recognition. *IEEE Transactions on Image Processing*, 23(12):5440–5454, 2014.
- [23] Olga Russakovsky, Jia Deng, Hao Su, Jonathan Krause, Sanjeev Satheesh, Sean Ma, Zhiheng Huang, Andrej Karpathy, Aditya Khosla, Michael Bernstein, et al. Imagenet large scale visual recognition challenge. *International journal of computer vision*, 115(3):211–252, 2015.
- [24] David Sandberg. Face recognition using tensorflow, April 2018.
- [25] Mark Sandler, Andrew Howard, Menglong Zhu, Andrey Zhmoginov, and Liang-Chieh Chen. Mobilenetv2: Inverted residuals and linear bottlenecks. In *Proceedings of the IEEE conference on computer vision and pattern recognition*, pages 4510–4520, 2018.
- [26] Florian Schroff, Dmitry Kalenichenko, and James Philbin. Facenet: A unified embedding for face recognition and clustering. In *Proceedings of the IEEE conference on computer vision and pattern recognition*, pages 815–823, 2015.
- [27] Christian Szegedy, Sergey Ioffe, Vincent Vanhoucke, and Alexander A Alemi. Inception-v4, inception-resnet and the impact of residual connections on learning. In *Thirty-First AAAI Conference on Artificial Intelligence*, 2017.
- [28] Mingtian Tan and Zhe Zhou. Do not return similarity: Face recovery with distance. *arXiv preprint arXiv:1901.09769*, 2019.
- [29] Y. Wang and J. Kato. Good choices for deep convolutional feature encoding. In *2019 IEEE Winter Conference on Applications of Computer Vision (WACV)*, pages 312–320, 2019.

- [30] Yandong Wen, Kaipeng Zhang, Zhifeng Li, and Yu Qiao. A discriminative feature learning approach for deep face recognition. In *European conference on computer vision*, pages 499–515. Springer, 2016.
- [31] Lior Wolf, Tal Hassner, and Itay Maoz. Face recognition in unconstrained videos with matched background similarity. In *CVPR 2011*, pages 529–534. IEEE, 2011.
- [32] Mengjia Yan, Mengao Zhao, Zining Xu, Qian Zhang, Guoli Wang, and Zhizhong Su. Vargfacenet: An efficient variable group convolutional neural network for lightweight face recognition. In *Proceedings of the IEEE International Conference on Computer Vision Workshops*, pages 0–0, 2019.
- [33] Dong Yi, Zhen Lei, Shengcai Liao, and Stan Z Li. Learning face representation from scratch. *arXiv preprint arXiv:1411.7923*, 2014.